Statics and Dynamics of 2D Colloidal Crystals in a Random Pinning Potential

Alexandros Pertsinidis* and Xinsheng Sean Ling†

Department of Physics, Brown University, Providence, Rhode Island 02912, USA

(Received 12 February 2007; revised manuscript received 17 August 2007; published 18 January 2008)

We report the first experimental study of a model system of a two-dimensional colloidal crystal in a random pinning potential. The colloidal crystal consists of monodispersed charged polystyrene microspheres suspended in deionized aqueous media and confined near a rough charged surface. It is found that the static orientational correlation function $g_6(r)$ decays exponentially for intermediate and strong pinning, in agreement with theories. The driven depinning is dominated by thermally activated creep motion along 1D-like channels between regions with short-range order. A coexistence model is proposed for describing the observations.

DOI: 10.1103/PhysRevLett.100.028303 PACS numbers: 82.70.Dd, 64.60.Ht, 83.50.Ha

Long-range order and rigidity are two closely related fundamental properties in condensed matter physics [1]. Often one can gain significant insights into the nature of order by studying the response of a system to a perturbing force. This well-established paradigm is faced with significant challenges when applied to systems with quenched disorder in the form of a static random potential landscape. It was pointed out in the seminal papers of Larkin [2] and of Imry and Ma [3] that true long-range order cannot survive in three-dimensional and two-dimensional systems with random pinning. As a result, there is always a complex interplay between elasticity and random pinning in statics and dynamics. Establishing a new paradigm in relating the driven dynamics to the structural order in random pinning systems is an important task.

The challenge is to identify and characterize the microscopic processes involved in the driven dynamics. In this Letter, we study a model system of 2D colloidal crystals. We report the first direct observation of the statics and dynamics of 2D colloidal crystals in a random substrate potential landscape created by microfabrication. It is found that the quasi-long-range order [4,5] of a 2D crystal is indeed destroyed as predicted by theories [2]. However, the dynamics of the system near the threshold of driven depinning show many interesting features characteristic of coexisting solid and liquid.

In this experiment, a monolayer of polystyrene microspheres, 0.36 μm in diameter, suspended in deionized water, was confined between two substrates, a quartz disk and a cover slip. For smooth surfaces, an ordered 2D colloidal crystal is formed (at room temperature) for a sufficient areal density of particles, due to the strong Coulomb repulsions. The areal density of the 2D system was $\approx 1.6\ \mu\mathrm{m}^{-1}$. The details of our sample cell can be found in [6,7]. To create a random pinning potential landscape, the quartz surface is roughened using a reactive-ion-etching technique [7]. To create samples of different pinning strengths *in situ* without changing other parameters of the colloidal suspension, several plateaus of different heights, differing by 500 nm, on the same substrate are fabricated (by ion-beam milling). It should be noted that the height difference is expressed as different separations d between the opposing surfaces (the pinning effects are more pronounced for smaller d, see below). (For $d > 2.5\ \mu$m, a bilayer square or hexagonal crystal forms.)

The rough surface results in a static pinning potential spatially varying with characteristic length scale of a few hundred nanometers, i.e., a few pinning sites per lattice spacing. Using video microscopy [8], one can determine the pinning potential landscape $V(\vec{x})$. For substrate separation $d = 1.0\ \mu$m, the characteristic energy scale of $V(\vec{x})$ is estimated [8] to be $E_0 \approx 0.4 k_B T$.

Figure 1 shows the statics of 2D colloidal crystals as a function of pinning strength. Both the pair distribution function $g(r)$ and the orientational correlation function $g_6(r)$ are shown. For an ordered state, $g(r)$ is sharply peaked at r values corresponding to magnitudes of lattice vectors. For the case of strong and intermediate disorder, at $d = 1.0$ and $1.5\ \mu$m, the pair distribution functions are liquidlike. For $d = 2.0\ \mu$m, the particles are further away from the confining walls, the particle-wall interaction is strongly screened, and the effective pinning potential is weak. As a result, $g(r)$ and $g_6(r)$ are characteristic of a 2D crystal.

The orientational order is quantified by the orientational correlation function $g_6(r) = \langle \psi_6(0)\psi_6^*(r)\rangle$, which is calculated using the bond-orientational order parameter field $\psi_6(\vec{x})$ [9]. For the ith particle, ψ_6 is defined as $\psi_6(\vec{x}_i) = \sum_j e^{-i6\theta_{ij}}$, where θ_{ij} denotes the angle of the line connecting nearest neighbors i and j. One expects $g_6(r) \sim e^{-r/\xi}$ for a disordered phase, and $g_6(r)$ approaches a nonzero value at large r for an ordered phase. For the disordered states ($d = 1.0$ and $1.5\ \mu$m), $g_6(r)$ shows exponential behavior, with $\xi = 1.6\ \mu$m and $\xi = 3.3\ \mu$m, corresponding to characteristic sizes of ordered regions of 2 and 4 lattice spacings, respectively. For $d = 2\ \mu$m, $g_6(r)$ is constant with r, indicating long-range orientational order (limited by the sample size).

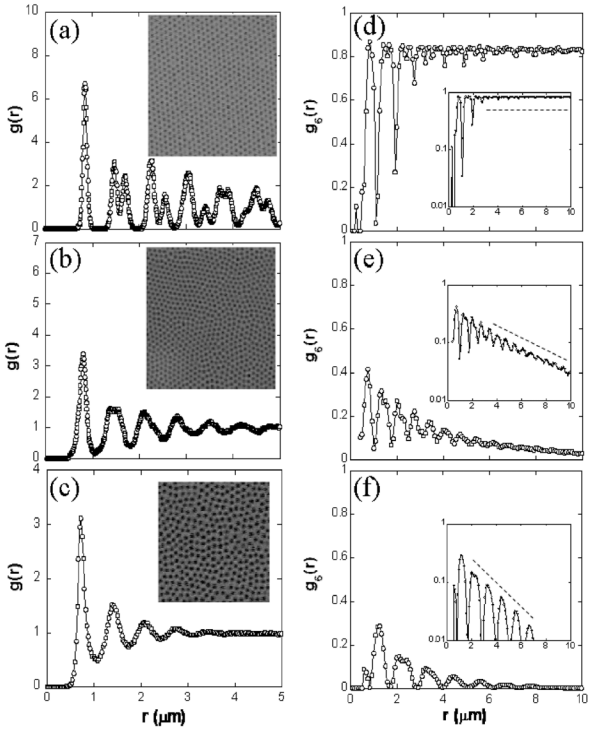

FIG. 1. (a)–(c) Pair distribution function $g(r)$. From top to bottom $d = 2.0$, 1.5, and 1.0 μm. Insets: Optical micrographs. (d)–(f) Orientational correlation function $g_6(r)$, calculated from $\psi_6(\vec{x})$ profiles. Insets in panels (d)–(f): Semilog plots of the same data. The dashed lines indicate the asymptotic behavior.

The exponential decay of $g_6(r)$ for $d = 1.0$ and 1.5 μm observed here is consistent with theories [10] that topological defects (dislocations and disclinations) will be induced by disorder. Figure 2 shows the typical defect structures observed at strong pinning for $d = 1.0$ μm. Clusters of edge dislocations and disclinations (fivefold and sevenfold coordinated particles) are randomly dispersed between misoriented crystallites of sixfold coordinated particles. Occasionally, one can identify a bound dislocation pair (shown in Fig. 2).

The fact that $g_6(r)$ is exponential for $d = 1.5$ μm, but remains constant for $d = 2.0$ μm, indicates disorder-induced melting. Our data can be used to provide a test of Larkin's collective pinning model [2] which predicts that the Larkin length $R_{\mathrm{LO}} = 2x^2\mu/(\sqrt{n}E_0)$, where μ is the shear modulus of the 2D crystal and x, n, and E_0 are the range, density, and characteristic energy scale of the pinning sites. At $d = 1.0$ μm, $x \approx 0.3$ μm, $E_0 = 0.4k_BT$, $\sqrt{n} \approx 1$ $\mu\mathrm{m}^{-1}$, and shear modulus $\mu \approx 10k_BT/\mu\mathrm{m}^2$, giving $R_{\mathrm{LO}} \approx 4.5$ μm in agreement (in order of magnitude) with the correlation length ξ.

Of particular interest is the response of the randomly pinned 2D lattice to an external driving force f. It was predicted [11] that there is a dynamical phase transition at a critical driving force f_c between pinned and moving phases at $T = 0$ for a purely elastic system. The average velocity is predicted to follow critical scaling as $v \sim (f - f_c)^\beta$, with $\beta = 2/3$ for a 2D elastic solid. At finite temperatures, one expects that the critical depinning should be preempted by thermally activated motion. In the collective creep model [12], the driven motion is facilitated by the creep of Larkin crystallites (or domains). However, recent numerical studies suggest a different kind of scenario for the depinning dynamics. For example, it has been found in numerical simulations that the depinning objects are linear channels [13,14].

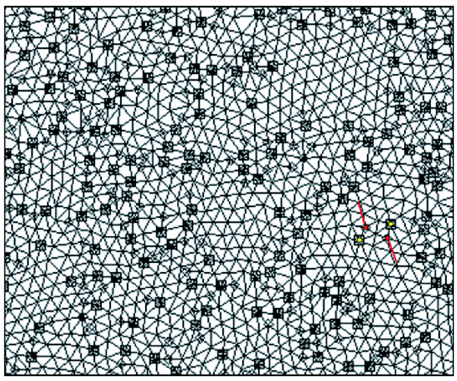

FIG. 2 (color online). Delaunay triangulation of a snapshot of video images of a colloidal lattice in strong random pinning, for $d = 1.0$ μm. The diamonds and squares represent fivefold and sevenfold coordinated particles (disclinations), respectively. A pair of edge dislocations is indicated by two solid (red) lines of two lattice spacings long on the right.

In our experiment, the 2D colloid layer is driven [15] by an electrical field. We typically applied 1–20 V on the electrodes spaced at about 5 mm (electric field 2–40 V/cm). In the case of weak pinning (ordered 2D lattice), the system exhibits elastic depinning, with the particles keeping the same neighbors as they move. For the strongly pinned disordered states, the system exhibits riverlike flow at the onset of motion. Figure 3 shows the trajectories of the particles near the threshold of depinning. A small fraction of particles is flowing in fractal-like channels around pinned islands. Each channel path does not repeat itself when the bias voltage is reset to zero and then turned back on. Thus the channel is not specific to a special path on the substrate.

At higher driving voltage, the flowing-river network becomes denser. We do occasionally observe, for intermediate disorder ($d = 1.5$ μm), behavior reminiscent of Larkin domain creep. In this case, the system is broken up into crystallites of size about 10 lattice spacings, during flow the crystallites do not break apart but maintain their connectivity, sliding past each other. However this behavior is more common at higher drive than close to the depinning threshold.

From the trajectories of the particles $\{\vec{x}_i\}$, we can obtain their velocities $\{\vec{v}_i\}$. Since we are interested in the drift velocity, we smoothed $\{\vec{x}_i\}$ with a moving average routine to minimize the effects of Brownian motion on the velocity

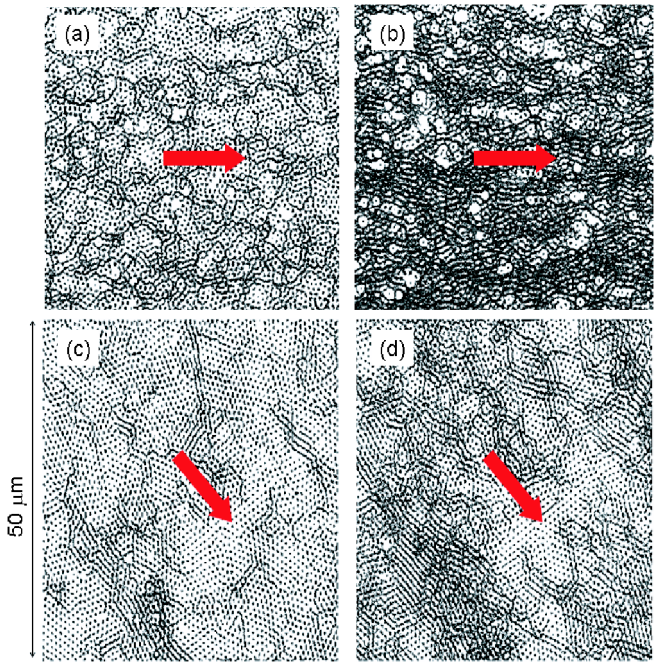

FIG. 3 (color online). Trajectories of particles showing the morphology of flow. (a),(b) Strong disorder ($d = 1.0$ μm), trajectories followed over 1.7 s. For (a) and (b), the driving voltages are 5 and 7 V, respectively. (c),(d) Intermediate disorder ($d = 1.5$ μm), trajectories followed over 1.7 s. For (c) and (d), the driving voltages are 6 and 9 V, respectively. The arrows indicate the direction of applied driving force.

data. The averaging window was typically 45 frames (0.75 s), but similar results are obtained with slightly different window size. In Fig. 4 we show the average velocity v of the particles as a function of the applied voltage. The curves were obtained by slowly ramping the voltage. For strong disorder, v is practically zero and it increases rapidly after a threshold voltage of order volts. The increase in v has a positive curvature. For weak disorder, the threshold is much smaller (order 0.1 V) and the v curve is rising with a negative curvature. In both cases, at large drive the velocity becomes linear to the applied force.

A striking observation is that, for a given drive voltage, e.g., 8 V, the velocity of the intermediate pinning state at $d = 1.5$ μm is much lower than that of the strong pinning state at $d = 1.0$ μm. The trajectory data in Fig. 3 offer a clue to this surprising result: for strong pinning, the individual moving channels populate the whole system, while at intermediate pinning, the moving particles are along channel-like paths, along the grain boundaries between the ordered domains which remain pinned.

We found that the $d = 1.0$ and 1.5 μm data in Fig. 4(a) cannot be fitted to a simple power-law form $v \sim (V - V_c)^\beta$ where V_c is the threshold voltage. Instead, we found an interesting exponential dependence of the average particle velocity on the driving voltage for both strong and intermediate pinning, at $d = 1.0$ and 1.5 μm. This behavior is

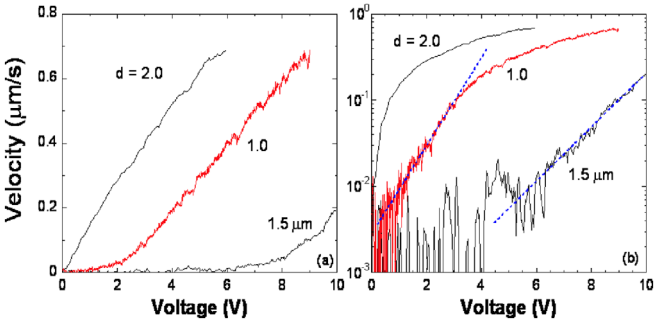

FIG. 4 (color online). (a) Average velocity versus applied voltage. Note that the velocity is a nonmonotonic function of separation d (and pinning strength, see text). (b) Semilog plots of data in (a).

reminiscent of the thermally activated flux creep phenomena in hard superconductors [18]. The exponential rise in velocity is due to a linear suppression of the pinning potential by the applied electric field. Thus we interpret the exponential dependence in Fig. 4(b) as evidence for ther-

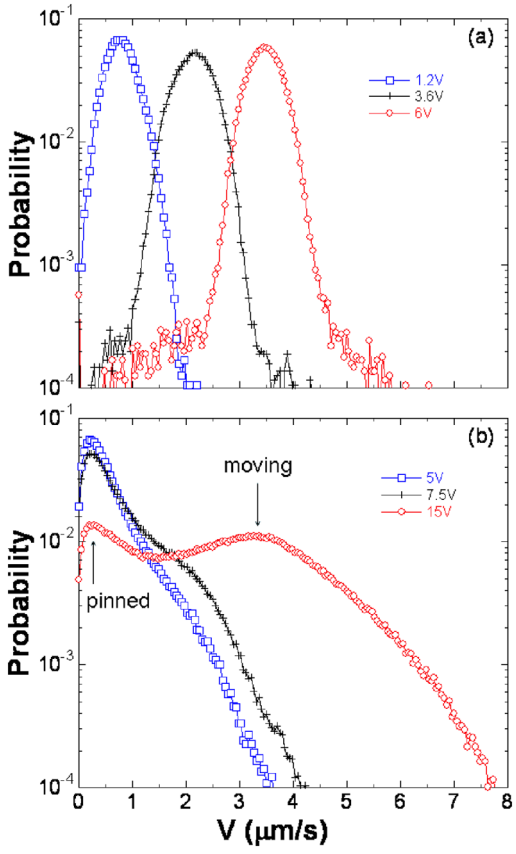

FIG. 5 (color online). Normalized velocity distributions as a function of the *amplitude* of velocity, at various driving voltages. (a) Weak pinning $d = 2.0$ μm, (b) strong pinning $d = 1.0$ μm. Note that in (a), for elastic flow, the velocity distribution is a single Gaussian centered at the average velocity. In (b), plastic flow, the distribution is bimodal, indicating coexisting pinned Larkin domains and moving channels.

mally activated creep dynamics of the particles flowing in the 1D-like channels between the Larkin domains as already implicated in the trajectory data in Fig. 3.

Another useful way to characterize the dynamic inhomogeneity of the depinning state is the probability distribution $P(v)$ of the velocities of the particles as introduced by Faleski, Marchetti, and Middleton [13]. The normalized probability distribution $P(v)$ is defined as $P(v) =$ histogram/sum(histogram), calculated after taking the histogram of the velocities over 1.5 s. The results for weak and strong pinning cases are shown in Fig. 5. Here v is the magnitude of the velocity, i.e., $v > 0$.

As shown in Fig. 5, for elastic flow, the velocities of the particles are peaked around a nonzero average velocity and the whole distribution is shifted to higher v with increasing drive. For plastic depinning, $P(v)$ is bimodal, with one peak at v close to zero, which is independent of driving force, and another peak at a finite v, corresponding to the pinned particles and moving particles, respectively. Because of Brownian motion of the pinned particles, the first peak is at a finite small value. The position of the second peak shifts to higher v for higher bias voltage V. The latter behavior is also seen in the simulations of Faleski, Marchetti, and Middleton [13].

The emerging physical picture here is that thermally activated depinning always occurs first along the 1D-like easy channels. When a 2D crystal is completely disordered by a strong random potential, the driven motion is that of thermally activated motion of individual particles. The system becomes fluidlike in statics and in motion. When a 2D crystal is partially disordered by random pinning, as in Fig. 3(c), the driven motion at the threshold of depinning is governed by the few individual particles moving along the grain boundaries separating the pinned ordered domains. The system appears to phase separate into fluidlike channels and pinned solid regions. We propose that it is perhaps useful to think of such systems as a coexistence phenomenon of coexisting solid, in the form of Larkin domains, and liquid in the form of Faleski-Marchetti-Middleton flow channels.

We wish to thank N. Daniilidis, J. M. Kosterlitz, M. C. Marchetti, Cynthia Olson, C. Reichhardt, and S. C. Ying for helpful discussions. This work was supported by NSF-DMR.

*Current address: QB3 Institute, University of California, Berkeley, CA 94720, USA.
†Corresponding author.
xsling@brown.edu.

[1] P. M. Chaikin and T. C. Lubensky, *Principles of Condensed Matter Physics* (Cambridge University Press, Cambridge, England, 1995).
[2] A. I. Larkin, Sov. Phys. JETP **31**, 784 (1970); A. I. Larkin and Yu. N. Ovchinnikov, J. Low Temp. Phys. **34**, 409 (1979).
[3] Y. Imry and S.-k. Ma, Phys. Rev. Lett. **35**, 1399 (1975).
[4] J. M. Kosterlitz and D. J. Thouless, J. Phys. C **6**, 1181 (1973).
[5] D. R. Nelson and B. I. Halperin, Phys. Rev. B **19**, 2457 (1979).
[6] A. Pertsinidis and X. S. Ling, Phys. Rev. Lett. **87**, 098303 (2001).
[7] A. Pertsinidis and X. S. Ling, New J. Phys. **7**, 33 (2005).
[8] We determine the pinning potential landscape $V(\vec{x})$ for substrate separation $d = 1.0$ μm by taking snapshots of the spatial distribution of a dilute concentration of particles. The probability of finding a particle in a region $d\vec{x}$ around $\vec{x}$ measures the local depth of the pinning potential. The strength of pinning sites follows an exponential distribution $D(V) \sim \exp(-V/E_0)$, with characteristic energy scale $E_0 \approx 0.4k_BT$. From typical pin size $x \sim$ 300 nm and the characteristic energy scale $E_0 \approx 0.4k_BT = 10^{-2}$ eV, we obtain a pinning force $f_p \approx \frac{E_0}{x} \sim 10^{-10}$ dyn. E_0 and f_p are expected to be reduce substantially with increasing d since the screened Coulomb interactions between the particle and the wall decreases rapidly with distance, as observed in our experiment.
[9] D. R. Nelson, in *Phase Transitions and Critical Phenomena*, edited by C. Domb and J. Lebowitz (Academic, London, 1983), Vol. 7, Chap. 1.
[10] D. Carpentier and P. Le Doussal, Phys. Rev. Lett. **81**, 1881 (1998).
[11] D. S. Fisher, Phys. Rev. B **31**, 1396 (1985).
[12] M. V. Feigel'man, V. B. Geshkenbein, A. I. Larkin, and V. M. Vinokur, Phys. Rev. Lett. **63**, 2303 (1989).
[13] M. C. Faleski, M. C. Marchetti, and A. A. Middleton, Phys. Rev. B **54**, 12427 (1996).
[14] C. Reichhardt and C. J. Olson, Phys. Rev. Lett. **89**, 078301 (2002).
[15] This is achieved by applying a voltage V between the two Ti/Au thin film electrodes, resulting in an electric field $E \sim O$ (V/cm) in the 2D region. Since the particles are negatively charged, they would drift with velocity $\mu_{ep}E$, where μ_{ep} is the electrophoretic mobility. Typically $\mu_{ep} \sim O$ (1–10) μm s^{-1}/(V cm^{-1}) for colloidal microspheres [16]. However, the Debye layer near the charged silica surface can carry counterion current, and fluid flow (due to drag) opposite to the particle drift arises in the 2D region. This electro-osmotic flow impedes particle drift, leading to a substantially reduced apparent mobility μ^* [17]. From the slope of the linear part of the velocity versus applied voltage for a driven 2D colloid, we estimate $\mu^* \sim 0.1$ μm s^{-1}/(V cm^{-1}). For overdamped motion, the force exerted on a particle equals the viscous drag force $f = 6\pi\eta a v$, and since $v = \mu^* E$, $f = 6\pi\eta a \mu^* E$, where η is fluid viscosity and a the Stokes radius. Using the measured mobility value, we estimate $f \sim 10^{-10}$ dyn (1 fN) for applied electric field $E \sim 1$ V/cm.
[16] M. Evers, N. Garbow, D. Hessinger, and T. Palberg, Phys. Rev. E **57**, 6774 (1998).
[17] R. J. Hunter, *Zeta Potential in Colloid Science* (Academic, London, 1981).
[18] P. W. Anderson, Phys. Rev. Lett. **9**, 309 (1962).